

# Combined XPS and DFT investigation of the adsorption modes of methyl enol ether functionalized cyclooctyne on Si(001)

Timo Glaser,<sup>[a]</sup> Jannick Meinecke,<sup>[b]</sup> Christian Länger,<sup>[a]</sup> Jan-Niclas Luy,<sup>[b, c, d]</sup> Ralf Tonner,<sup>[b, c, d]</sup> Ulrich Koert,<sup>[b]</sup> and Michael Dürr\*<sup>[a]</sup>

The reaction of methyl enol ether functionalized cyclooctyne on the silicon (001) surface was investigated by means of X-ray photoelectron spectroscopy (XPS) and density functional theory (DFT). Three different groups of final states were identified; all of them bind on Si(001) via the strained triple bond of cyclooctyne but they differ in the configuration of the methyl enol ether group. The majority of molecules adsorbs without

additional reaction of the enol ether group; the relative contribution of this configuration to the total coverage depends on substrate temperature and coverage. Further configurations include enol ether groups which reacted on the silicon surface either via ether cleavage or enol ether groups which transformed on the surface into a carbonyl group.

## 1. Introduction

Well-defined structures of organic molecules on semiconductors, in particular on Si(001) as the technologically most important semiconductor surface, may open new possibilities in semiconductor technology with its wide range of applications.<sup>[1–7]</sup> One prerequisite for the formation of such well-defined organic structures is the chemoselective attachment of bifunctional molecules. However, due to the high reactivity of the dangling bonds, only a few bifunctional molecules have been shown to exhibit chemoselective reactivity on Si(001),<sup>[8–12]</sup> often restricted to a fixed combination of the two functional groups.

A more general concept is based on cyclooctynes, which are well known from click chemistry.<sup>[13,14]</sup> Previous investigations have shown that substituted cyclooctynes selectively react on

Si(001) over the strained triple bond of the cyclooctyne ring.<sup>[15–17]</sup> The chemoselective reactivity of substituted cyclooctynes was traced back to the direct reaction pathway of cyclooctyne on Si(001),<sup>[15,18,19]</sup> in contrast to almost all other organic functional groups, which adsorb on Si(001) via an indirect reaction channel.<sup>[3,5]</sup> In consequence, the second functional group of the substituted cyclooctynes was found not to take part in the adsorption process<sup>[15–17]</sup> and thus can be used for further reactions.

In this context, methyl enol ether functionalized cyclooctyne (MEECO, **1**, Figure 1) is a promising molecule to build the first organic layer on the silicon surface via the strained triple bond. The enol ether group could then be employed in click reactions with tetrazine derivatives,<sup>[20]</sup> which opens up a new way of building well-ordered multilayers on the silicon substrate. It is thus important to investigate the reaction of MEECO on Si(001), in particular with respect to the reaction of the enol ether group with the silicon surface.

Here we use X-ray photoelectron spectroscopy (XPS) and density functional theory (DFT) in order to investigate the

- [a] T. Glaser, Dr. C. Länger, Prof. Dr. M. Dürr  
Institut für Angewandte Physik und Zentrum für Materialforschung,  
Justus-Liebig-Universität Giessen,  
Heinrich-Buff-Ring 16, D-35392 Giessen, Germany  
E-mail: michael.duerr@ap.physik.uni-giessen.de
- [b] J. Meinecke, J.-N. Luy, Prof. Dr. R. Tonner, Prof. Dr. U. Koert  
Fachbereich Chemie, Philipps-Universität Marburg, Hans-Meerwein-Straße  
4, D-35032 Marburg, Germany
- [c] J.-N. Luy, Prof. Dr. R. Tonner  
Fakultät für Chemie und Pharmazie,  
Universität Regensburg, Universitätsstraße 31,  
D-93053 Regensburg, Germany
- [d] J.-N. Luy, Prof. Dr. R. Tonner  
Wilhelm-Ostwald-Institut für Physikalische und Theoretische Chemie,  
Universität Leipzig, Linnéstraße 2,  
D-04103 Leipzig, Germany

Supporting information for this article is available on the WWW under  
<https://doi.org/10.1002/cphc.202000870>

© 2020 The Authors. ChemPhysChem published by Wiley-VCH GmbH.  
This is an open access article under the terms of the Creative Commons  
Attribution Non-Commercial NoDerivs License, which permits use and  
distribution in any medium, provided the original work is properly cited,  
the use is non-commercial and no modifications or adaptations are  
made.

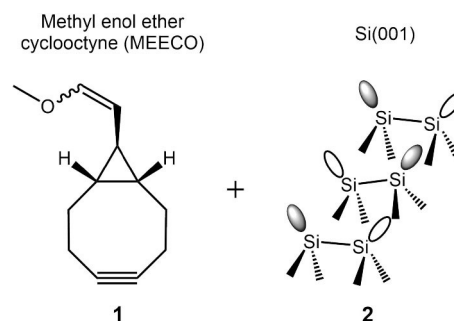


**Figure 1.** The adsorption of methyl enol ether functionalized cyclooctyne (MEECO, **1**) on the buckled dimers of Si(001) (**2**) is investigated. The latter are shown with filled dangling bonds (grey ellipses) and unfilled dangling bonds (white ellipses).<sup>[3,4]</sup>

adsorption configurations of methyl enol ether functionalized cyclooctyne at different temperature and coverage.

## Methods

The XPS experiments were performed in a UHV chamber with a base pressure  $< 1 \times 10^{-10}$  mbar. Si(001) samples were prepared by degassing at 700 K and repeated direct current heating cycles to 1450 K. A well ordered  $2 \times 1$  reconstruction was obtained by cooling with rates of about 1 K/s.<sup>[21,22]</sup>

The synthesis of MEECO was carried out via 8 linear steps leading into a yield of 32 %, consisting of a mixture of 64 % E-isomer and 36 % Z-isomer. The functionalization of the cyclooctyne ring was carried out using copper mediated cyclopropanation.<sup>[20]</sup> Methyl enol ether functionalized cyclooctyne was dosed via a leak valve from the vapor phase in a test tube. Pressures are given as uncorrected ion-gauge readings.

XPS measurements were performed using an Al  $K_{\alpha}$  X-ray source with monochromator (Omicron XM1000) and a hemispherical energy analyzer (Omicron EA125). All XPS spectra were referenced to the Si 2p<sub>3/2</sub> peak at 99.4 eV.<sup>[23]</sup> Voigt-profiles were used for fitting the data; they are composed of 90 % Gaussian function and 10 % Lorentzian function. Full width at half maximum (FWHM) of the single components was chosen between 0.9 and 1.1 eV, which are typical values for the measured line widths of such systems in this setup.<sup>[24]</sup>

DFT investigations were done with the Vienna ab initio simulation package (VASP 5.4.4)<sup>[25–27]</sup> using the HSE06<sup>[28]</sup> range-separated hybrid functional and standard PAW-pseudopotentials PBE.54<sup>[29]</sup> with a large core configuration while dispersion effects were considered via the DFT-D3 scheme including an improved damping function.<sup>[30,31]</sup> The plane wave energy cutoff was set to 400 eV and a total energy difference of at least  $10^{-6}$  eV with “accurate” precision was used for SCF convergence. Prior structural optimization was performed with the PBE<sup>[32]</sup> generalized gradient approximation including DFT-D3 correction and a force convergence criterion of  $10^{-2}$  eV. Transition-state structures were calculated with the dimer method<sup>[33]</sup> as implemented in the transition state tools (1.73) for VASP with tighter electronic convergence of  $10^{-7}$  eV. A  $\Gamma$ -centered  $2 \times 2 \times 1$   $k$ -mesh was chosen together with a setup of Si(001) slabs (six layers, two bottom layers frozen and terminated with hydrogen atoms) as determined in previous work.<sup>[34]</sup> Thermodynamic corrections were determined in a constrained Hessian approach at the PBE-D3 level with only the adsorbate and the two topmost slab layers being considered for displacements in finite difference calculations. The free energy differences at 300 K and 1 bar were then added as a higher order correction to the HSE06-D3 energies. Scripts for extracting thermodynamic quantities from a VASP calculation have been published elsewhere.<sup>[23]</sup> We will discuss electronic energy differences and Gibbs energies of adsorption at the HSE06-D3 level of approximation unless otherwise noted. PBE-D3 values are found in the Supporting Information (Figures S2 and S3).

## 2. Results and Discussion

In Figure 2, XPS spectra measured directly after adsorption of MEECO ( $3.5 \times 10^{-6}$  mbar $\times$ s) on Si(001) at 150 K as well as after a further temper cycle to 300 K are compared. Initial adsorption at 150 K led to the formation of a multilayer shown in light purple; the intensity is scaled by a factor of  $\approx 0.5$  for better

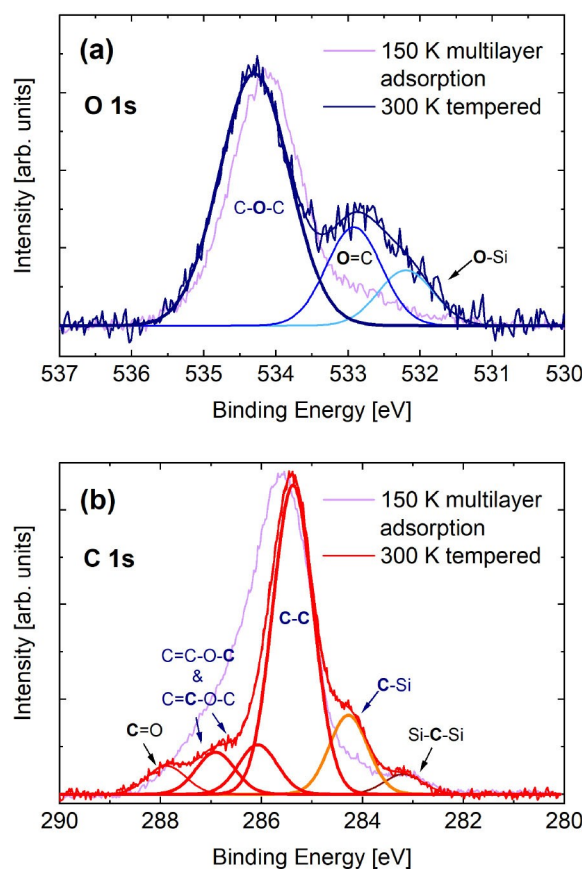


**Figure 2.** O 1s (a) and C 1s (b) core level spectra after adsorption of MEECO on Si(001) at 150 K. The light purple data were measured right after adsorption at 150 K. The O 1s and C 1s spectra in blue and red, respectively, were measured at 150 K after tempering the sample to 300 K within 30 minutes. The initial 150-K-spectra are higher in intensity indicating adsorption of a multilayer; they were scaled by a factor of  $\approx 0.5$  for better comparison with the spectra measured on the tempered sample. Fit components which are associated with the intact MEECO molecules attached via the strained triple bond are drawn with thick solid lines and are labelled dark blue. Further fit components are shown with thin solid lines. Decomposition of the multilayer spectra is shown in Figure S1 in the Supporting Information.

comparison with the data of the tempered sample, which are shown in blue (Figure 2 (a), O 1s) and red (Figure 2 (b), C 1s). The O 1s spectrum taken after the temper cycle (Figure 2 (a)) indicates three different peaks. The peak at the highest binding energy (534.3 eV, fit component shown in dark blue) can be assigned to the intact methyl enol ether group, as it coincides with the most dominant peak in the multilayer spectrum. In comparison with data reported in literature, the peak at 532.8 eV (azure fit component) can be assigned to a carbonyl group<sup>[35,36]</sup> and the third peak, indicated by the light blue component at a binding energy of 532.2 eV, can be assigned to an oxygen atom binding to the silicon surface.<sup>[24,37–39]</sup> This Si–O configuration indicates that an ether cleavage reaction took place on the surface.<sup>[39]</sup> The relative intensities of the O 1s components in the spectrum shows that the majority of the methyl enol ether groups stays intact when the molecule adsorbs on the Si(001) surface, while side reactions forming

C=O and Si–O bonds can take place. The intensity ratio of the three components is approx. 6:2:1.

The C 1s spectrum taken after the temper cycle shows six different peaks. The peak with the highest intensity at 285.4 eV can be assigned to C–C or C–H configurations, which are present in the main unit of the molecule.<sup>[15,17,36]</sup> The peak at a binding energy of 284.2 eV can be assigned to carbon atoms bonding via one covalent bond to the Si surface.<sup>[15,36,39]</sup> The fitted component is highlighted in orange in Figure 2. The intensity ratio of this component with respect to the total intensity of the carbon spectrum indicates that approximately 2 out of 12 carbon atoms are bonding in that mode on the Si surface.

The peaks at lowest and highest binding energy, 283.2 eV (dark red component) and 287.9 eV, are assigned to a C atom bound more strongly to the silicon substrate, e.g., via two Si dimer atoms as in disiliranes,<sup>[36,40]</sup> and a C atom in a carbonyl group,<sup>[35,36]</sup> respectively. The two remaining peaks at a binding energy of 286.0 eV and 286.9 eV are then assigned to the intact methyl enol ether group (C=C–O–C and C=C–O–C,<sup>[15]</sup>), in accordance with the O 1s spectrum, which also indicates a strong contribution of the intact enol ether group to the signal. Indeed, the relative intensity of each of these two peaks amounts to approx. 1/12 of the total intensity, indicating that the majority of the enol ether groups were not reacted.

When taking into account the different relative sensitivity factors for the O 1s and C 1s signals, an intensity ratio of 1.1:12 for I(O):I(C) was deduced for the spectra of the tempered sample, in accordance with the 1:12 ratio of the number of oxygen and carbon atoms in the MEECO molecule.

Furthermore, taking into account that most of the molecules bound to the surface exhibit an intact enol ether group as deduced from the O 1s and C 1s spectra, the ratio of 2:12 between the C–Si peak intensity and the total carbon intensity is a strong indication that most MEECO molecules bind via the strained triple bond of the cyclooctyne ring. However, the enol ether groups which react via ether cleavage also contribute to the Si–C peak intensity. It is thus possible that some of the MEECO molecules bind via the Si–O bond of the reacted enol ether group only; within the uncertainty of our measurements, we can neither exclude nor safely confirm such a bonding via the cleaved enol ether group only. On the other hand, a substantial contribution of molecules which additionally adsorb via the activated C=C bond of the enol ether group can be largely excluded as they would lead to a further increase of the intensity of the C–Si peak.

We thus propose three different groups of adsorption products as summarized in Figure 3: (a) MEECO bound to Si(001) solely via the strained triple bond of cyclooctyne, thus exhibiting an intact enol ether group. (b) MEECO bound via the strained triple bond of cyclooctyne and a further reaction via the ether group. One possible configuration for the respective product is sketched in Figure 3 (b) with the oxygen atom and an additional CH<sub>3</sub> group bound to the surface. C–O cleavage could also take place at the C–O bond next to the C=C double bond leading to an adsorbed methoxy group. As both configurations contribute in a similar way to the XPS spectra,

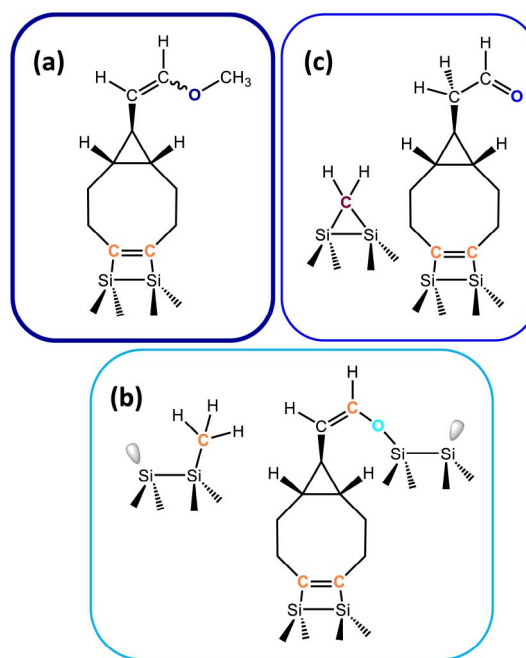


**Figure 3.** Three different adsorption configurations of MEECO on Si(001). (a) Adsorption via the cyclooctyne ring only. (b) Including an additional covalent Si–O bond due to ether cleavage. In the shown example, ether cleavage leads to a CH<sub>3</sub> group adsorbed on an additional Si dimer as observed for cyclooctyne ether.<sup>[15]</sup> (c) Including a carbonyl group in the former MEECO molecule and the resulting CH<sub>2</sub> fragment bound to two silicon atoms.

we cannot distinguish the two modes experimentally. (c) MEECO bound via the strained triple bond of cyclooctyne and the enol ether group being reacted to a carbonyl group.

Two further XPS measurements are shown in Figure 4. The spectra shown in Figure 4 (a) represent a Si(001) surface saturated with MEECO at room temperature (coverage  $\Theta = \Theta_{\text{sat}}$ ). The spectra shown in Figure 4 (b) were obtained at 150 K with a MEECO coverage below  $\Theta_0$ , the coverage which we obtained when tempering a multilayer to 300 K after adsorption at 150 K (compare Figure 2).  $\Theta_0$  is  $\approx 50\%$  higher than the saturation coverage of MEECO molecules on the surface at  $T_s = 300$  K. All peaks observed in the measurements shown in Figure 2 are also observed in the spectra in Figure 4. At 150 K, an additional peak at 535.1 eV can be observed. It is assigned to a dative O–Si bond of the oxygen atom of the methyl enol ether group.<sup>[39]</sup> In this configuration, the enol ether group is still intact; if we combine the intensity of this component with the intensity of the component assigned to the free enol ether group, the majority of molecules adsorb with an intact enol ether group at low coverage, as well. However, compared to the measurement shown in Figure 2, the ratio is shifted towards molecules which reacted via ether cleavage or carbonyl formation. In particular, the relative intensity of the peak assigned to the carbonyl peak in the O 1s spectrum shows the highest intensity of all single peaks. At 300 K, the ratio of intact methyl enol ether groups compared to reacted groups is then favouring the reacted groups; the signal associated with oxygen

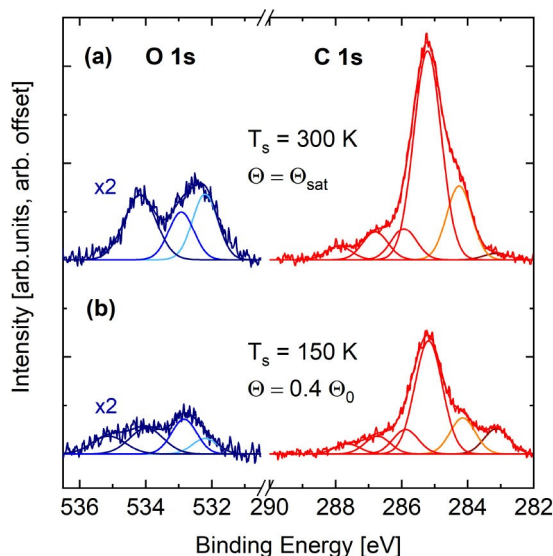


**Figure 4.** O 1s spectra shown in blue and C 1s spectra shown in red of methyl enol ether functionalized cyclooctyne on Si(001) after adsorption at 300 K (a) and 150 K (b). At 150 K, an additional peak at 535.1 eV can be observed when compared to Figure 1 (a), which is assigned to a dative O–Si bond of the methyl enol ether group to Si(001).<sup>[39]</sup> Further peak assignments are identical to Figure 1. The O 1s spectra are scaled by a factor 2 for better comparison.

bonding to the silicon surface (light blue) is slightly increased compared to the signal of the carbonyl group (azure).

The relative contribution of the different configurations as deduced from the intensity of the different oxygen species is summarized in Figure 5. The data include adsorption and measurement at 150 K (dashed box), adsorption and measurement at 300 K (dotted box), and measurements of a sample prepared at 150 K and further tempered to 300 K (also measured at 150 K, dot-dashed box). Oxygen atoms bonding

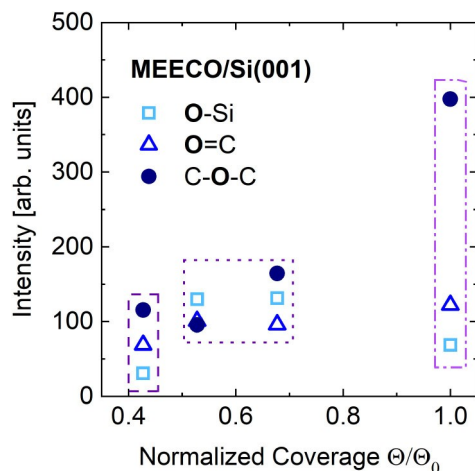


**Figure 5.** Intensity of the different oxygen species of the methyl enol ether group as measured for different surface coverage and adsorption/measurement temperature: adsorption and measurement at 150 K (dashed box), adsorption and measurement at 300 K (dotted box), adsorption at 150 K and further tempering to 300 K (also measured at 150 K, dot-dashed box).

covalently with the Si(001) surface and the carbonyl group are formed with high relative contribution at 300 K and low coverage on the surface, indicating a high probability for cleavage of the methyl enol ether group at these conditions. At high coverage and reduced temperature, the reaction of the enol ether group with the surface is suppressed. In particular, ether cleavage is suppressed at lower temperatures, in accordance with previous work on the reaction of ether-functionalized cyclooctynes on Si(001).<sup>[15,41]</sup> With the latter preparation scheme (multilayer adsorption at 150 K, tempering to 300 K), the highest contribution of intact MEECO molecules to the total coverage was obtained (approx. 70% as deduced from the O 1s spectra in Figure 2 (a)).

The three types of bonding configurations shown in Figures 3 (a) to (c) are deduced from the assignment of the single components found in the O 1s and C 1s spectra at different surface coverage and temperature. Although all three configurations seem to be plausible with respect to the adsorption of the single functional groups, i. e., strained triple bond and enol ether group, it is not clear if they can react in this way when combined in one single molecule. Furthermore, the relative contribution of the side reactions is dependent on both coverage and temperature. The latter might be caused either by kinetic or thermodynamic control. We thus performed DFT calculations to reveal more details about the possible adsorption modes.

The most stable adsorption modes found in the computational investigations are shown in Figures 6 (a) to (d). They reflect the configurations shown in Figure 3, explicitly taking into account two possibilities for O–C cleavage in combination with the formation of a Si–O bond. They show large adsorption energies throughout, indicating strong chemisorption, with

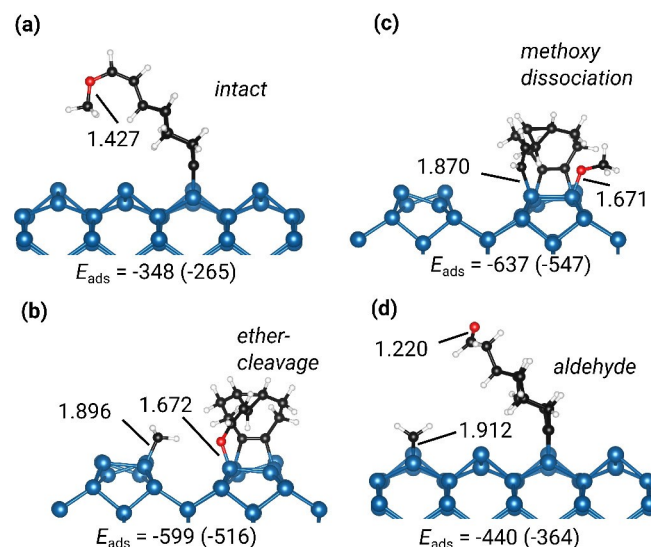


**Figure 6.** Results from DFT studies. (a) to (d): Most important adsorption modes with adsorption energies (HSE06-D3) given in kJ mol<sup>−1</sup> (Gibbs free energy in brackets). Selected bond distances are given in Å. In (b) and (c), the silicon substrate is rotated by 90° with respect to the situation shown in (a) and (d). In Figure S4 in the Supporting Information, the rotated view of (a) is also shown.



rather constant contributions from enthalpic and entropic effects (Gibbs energies are given in brackets). Regarding the mix of stereoisomers used in the experimental study, we find that the *E*-isomer of free MEECO is more stable by  $17 \text{ kJ mol}^{-1}$  compared to the *Z*-isomer. We find the same adsorption modes for both isomers, however the *Z*-isomer binds more strongly to the surface and those structures are thus depicted in Figures 6 (a) and (b). The *E*-isomer is less strongly bound (*intact* mode:  $\Delta E_{\text{ads}}^{\text{PBE-D3}} = +6 \text{ kJ mol}^{-1}$ , *ether-cleavage* mode:  $\Delta E_{\text{ads}}^{\text{PBE-D3}} = +52 \text{ kJ mol}^{-1}$ ) but it seems reasonable to assume that both isomers will react in the same manner with the surface. All adsorption energies are given with respect to the energy of the respective isomer.

The *intact* adsorption mode is very similar to the *on-top* structure for parent cyclooctyne which shows exactly the same adsorption energy at PBE level ( $E_{\text{ads}}^{\text{PBE-D3}} = -308 \text{ kJ mol}^{-1}$ , [42]). This supports the previous finding that the substitution of cyclooctyne in the backbone does not have an influence on the bonding to the substrate. [16] The adsorbate can further react via breaking the C–O bond at the ether group via the previously observed  $S_N2$ -type attack [43] of a silicon atom in the neighboring dimer row leading to the strongly bound adsorption mode *ether-cleavage*. Like in the previous investigation, breaking of the C–O bond proceeds via an intermediate state with the intact ether group being datively bonded to the surface dimer. The adsorption energy for the final state is comparable to the doubly-bonded configuration of an ether-functionalized cyclooctyne (5-ethoxymethyl-5-methylcyclooctyne, EMC) with the triple bond attached to the surface and the ether bond cleaved across the dimer rows (*ether-cleavage*:  $E_{\text{ads}}^{\text{PBE-D3}} = -540 \text{ kJ mol}^{-1}$ , EMC:  $E_{\text{ads}}^{\text{PBE-D3}} = -557 \text{ kJ mol}^{-1}$  [16]).

An alternative to the *ether-cleavage* reaction across dimer rows is O–C cleavage via the *methoxy dissociation* mode (Figure 6 (c)). Here, we also find a very stable structure with  $E_{\text{ads}} = -637 \text{ kJ mol}^{-1}$ . This cleavage reaction is preferred on-top of the same dimer in contrast to the ether cleavage reaction across rows.

The fourth important structure found is the *aldehyde* mode (Figure 6 (d)), which shows an increased adsorption energy compared to *intact* due to the additional methylene group bonding to the surface. Here, a tautomeric enol-configuration can be envisioned which turns out to be less stable by  $\Delta E = 25 \text{ kJ mol}^{-1}$ . In the XPS spectra, this tautomerism would lead to a lower intensity of the C=O signal when compared to the Si–C–Si signal, which is only observed in the low coverage measurement performed at 150 K (Figure 4 (b)). Indeed, the tautomeric enol-configuration might serve as an intermediate in the reaction towards the *aldehyde* mode. However, as the respective pathway is not obvious, a full computational description is beyond the scope of this investigation.

There are further possibilities for MEECO to react with Si(001) which have been investigated computationally. We find that the adsorption via the ether oxygen only (dative bond) shows adsorption energies of  $E_{\text{ads}}^{\text{PBE-D3}} = -91 / -86 \text{ kJ mol}^{-1}$  (*Z*/*E*) which is considerably lower compared to previously investigated ether dative bonds on Si(001) (tetrahydrofuran:  $E_{\text{ads}}^{\text{PBE-D3}} = -132 \text{ kJ mol}^{-1}$ ; diethylether:

$E_{\text{ads}}^{\text{PBE-D3}} = -116 \text{ kJ mol}^{-1}$  [43]). Bonding analysis with an energy decomposition method for extended systems (pEDA) [44] indicates that this is due to reduced donation from the non-bonded electron pairs into the acceptor orbitals at the surface ( $\Delta E_{\text{orb}}^{\text{donation}}(\text{PBE-D3}) = 198 \text{ kJ mol}^{-1}$  compared to  $\Delta E_{\text{orb}}^{\text{donation}}(\text{PBE-D3}) = 284 \text{ kJ mol}^{-1}$  for diethylether [43]) due to increased conjugation with the double bond. As found for EMC before, this dative bond can thus be excluded as final state but plays a role as intermediate as outlined above. [15]

The third functional group in MEECO is the double bond. Adsorption via this double bond alone leads to a reasonably stable structure for the *E*-isomer ( $E_{\text{ads}} = -231 \text{ kJ mol}^{-1}$ ) which is nevertheless much less stable compared to the adsorption via the triple bond. Adsorption via both functional groups – double and triple bond – has also been tested and the most stable configuration (triple bond in bridge-configuration and double bond in on-top configuration on neighboring dimer row) results in  $E_{\text{ads}} = -462 \text{ kJ mol}^{-1}$  (*Z*) and  $E_{\text{ads}} = -454 \text{ kJ mol}^{-1}$  (*E*). It is thus comparable to the *intact* and *aldehyde* modes. Nevertheless, this mode can be excluded based on the XPS findings that a rather low ratio of signal intensity in the C 1s spectrum is associated with C–Si bonds.

Finally, we computed the energy barrier for the reaction from *intact* to *ether-cleavage* structure via the datively bonded intermediate (Figure 7) in analogy to previously investigated ether cleavage reactions on Si(001). [16,43] A moderate barrier of  $\Delta E^\ddagger = 79 \text{ kJ mol}^{-1}$  was calculated. For the alternative reaction of methoxy cleavage, a higher barrier was found ( $\Delta E^\ddagger = 102 \text{ kJ mol}^{-1}$ ). These calculated barriers support the experimental observation that reduced reaction via ether cleavage is found in the low temperature measurements but MEECO reacts more readily via the enol ether group upon increasing the temperature. In addition, if at reduced temperature the reaction rate is low when compared to the flux of the incoming molecules, site blocking can further reduce the number of molecules additionally reacted via the enol ether group, in particular at high coverage.

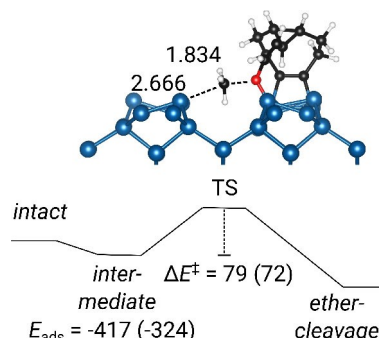


**Figure 7.** Reaction path of the MEECO molecule bound in the *intact* configuration to the *ether-cleavage* structure via the datively bonded intermediate. The transition state configuration is shown with barrier height ( $\Delta E^\ddagger$ , Gibbs energy in brackets). Selected bond distances are given in Å, energies in  $\text{kJ mol}^{-1}$ .

### 3. Conclusion

Preferential adsorption of MEECO molecules via the strained triple bond of cyclooctyne has been experimentally observed at 150 K. Increased substrate temperature leads to additional products via reaction of the enol ether group, i.e., ether cleavage leading to a Si-bound oxygen atom or the formation of a carbonyl group in the former MEECO molecule. DFT-based computational investigations support the bonding configurations proposed from XPS. They furthermore rationalize the experimental findings as they find a lower adsorption energy for the MEECO molecules bound solely via the strained triple bond when compared to multi-tethered molecules but, where calculated, a finite reaction barrier into these thermodynamically preferred configurations.

### Supporting Information

The Supporting Information includes O 1s and C 1s spectra and their decomposition of a MEECO multilayer adsorbed at 150 K on Si(001) as well as additional results from DFT calculations and information on the computational raw data.

### Acknowledgement

We acknowledge financial support by the Deutsche Forschungsgemeinschaft through SFB 1083 (project-ID 223848855) and DU 1157/4-1. We thank HRZ Marburg, GOETHE-CSC Frankfurt and HLR Stuttgart for computational resources. Open access funding enabled and organized by Projekt DEAL.

### Conflict of Interest

The authors declare no conflict of interest.

**Keywords:** chemoselective adsorption • density functional calculations • organic molecules • silicon surface • X ray photoelectron spectroscopy

- [1] J. T. Yates Jr., *Science* **1998**, 279, 335–336.
- [2] R. A. Wolkow, *Annu. Rev. Phys. Chem.* **1999**, 50, 413–41.
- [3] M. A. Filler, S. F. Bent, *Prog. Surf. Sci.* **2003**, 73, 1–56.
- [4] J. Yoshinobu, *Prog. Surf. Sci.* **2004**, 77, 37–70.
- [5] T. R. Leftwich, A. V. Teplyakov, *Surf. Sci. Rep.* **2008**, 63, 1–71.
- [6] F. F. Tao, Y. Zhu, S. L. Bernasek in *Functionalization of Semiconductor Surfaces*, John Wiley and Sons Inc., Hoboken, New Jersey, **2012**.
- [7] A. V. Teplyakov, S. F. Bent, *J. Vac. Sci. Technol. A* **2013**, 31, 050810.
- [8] M. Hossain, Y. Yamashita, K. Mukai, J. Yoshinobu, *Chem. Phys. Lett.* **2004**, 388, 27–30.

- [9] Y. X. Shao, Y. H. Cai, D. Dong, S. Wang, S. G. Ang, G. Q. Xu, *Chem. Phys. Lett.* **2009**, 482, 77–80.
- [10] M. Ebrahimi, K. Leung, *Surf. Sci.* **2009**, 603, 1203–1211.
- [11] Y. P. Zhang, J. H. He, G. Q. Xu, E. S. Tok, *J. Phys. Chem. C* **2011**, 115, 15496–15501.
- [12] B. Shong, T. E. Sandoval, A. M. Crow, S. F. Bent, *J. Phys. Chem. Lett.* **2015**, 6, 1037–1041.
- [13] M. F. H. C. Kolb, K. B. Sharpless, *Angew. Chem. Int. Ed.* **2001**, 40, 2004–2021; *Angew. Chem.* **2001**, 113, 2056–2075.
- [14] N. Münster, P. Nikodemak, U. Koert, *Org. Lett.* **2016**, 18, 4296–4299.
- [15] M. Reutzel, N. Münster, M. A. Lipponer, C. Länger, U. Höfer, U. Koert, M. Dürr, *J. Phys. Chem. C* **2016**, 120, 26284–26289.
- [16] L. Pecher, R. Tonner, *Theor. Chem. Acc.* **2018**, 137, 48.
- [17] C. Länger, J. Heep, P. Nikodemak, T. Bohamud, P. Kirsten, U. Höfer, U. Koert, M. Dürr, *J. Phys. Condens. Matter* **2019**, 31, 034001.
- [18] G. Mette, M. Dürr, R. Bartholomäus, U. Koert, U. Höfer, *Chem. Phys. Lett.* **2013**, 556, 70–76.
- [19] L. Pecher, S. Schmidt, R. Tonner, *J. Phys. Chem. C* **2017**, 121, 26840–26850.
- [20] J. Meinecke, U. Koert, *Org. Lett.* **2019**, 21, 7609–7612.
- [21] M. Dürr, Z. Hu, A. Biedermann, U. Höfer, T. F. Heinz, *Phys. Rev. B* **2001**, 63, 121315.
- [22] G. Mette, C. Schwalb, M. Dürr, U. Höfer, *Chem. Phys. Lett.* **2009**, 483, 209–213.
- [23] J. Heep, J.-N. Luy, C. Langer, J. Meinecke, U. Koert, R. Tonner, M. Dürr, *J. Phys. Chem. C* **2020**, 124, 9940–9946.
- [24] C. Länger, T. Bohamud, J. Heep, T. Glaser, M. Reutzel, U. Höfer, M. Dürr, *J. Phys. Chem. C* **2018**, 122, 14756–14760.
- [25] G. Kresse, J. Hafner, *Phys. Rev. B* **1993**, 47, 558–561.
- [26] G. Kresse, J. Furthmüller, *Comput. Mater. Sci.* **1996**, 6, 15–50.
- [27] G. Kresse, J. Furthmüller, *Phys. Rev. B* **1996**, 54, 11169–11186.
- [28] A. V. Krukau, O. A. Vydrov, A. F. Izmaylov, G. E. Scuseria, *J. Chem. Phys.* **2006**, 125, 224106.
- [29] G. Kresse, D. Joubert, *Phys. Rev. B* **1999**, 59, 1758–1775.
- [30] S. Grimme, J. Antony, S. Ehrlich, H. Krieg, *J. Chem. Phys.* **2010**, 132, 154104.
- [31] S. Grimme, S. Ehrlich, L. Goerigk, *Comput. Mater. Sci.* **2011**, 32, 1456–1465.
- [32] J. P. Perdew, K. Burke, M. Ernzerhof, *Phys. Rev. Lett.* **1996**, 77, 3865–3868.
- [33] G. Henkelman, H. Jonsson, *J. Chem. Phys.* **1999**, 111, 7010–7022.
- [34] J. Pecher, R. Tonner, *ChemPhysChem* **2017**, 18, 34–38.
- [35] J. L. Armstrong, J. M. White, M. Langell, *J. Vac. Sci. Technol. A* **1997**, 15, 1146–1154.
- [36] K. M. O'Donnell, C. Byron, G. Moore, L. Thomsen, O. Warschkow, A. Teplyakov, S. R. Schofield, *J. Phys. Chem. C* **2019**, 123, 22239–22249.
- [37] H.-N. Hwang, J. Y. Baik, K.-S. An, S. S. Lee, Y. Kim, *J. Phys. Chem. B* **2004**, 108, 8379–8384.
- [38] G. Mette, M. Reutzel, R. Bartholomäus, S. Laref, R. Tonner, M. Dürr, U. Koert, U. Höfer *ChemPhysChem* **2014**, 15, 3725–3728.
- [39] M. Reutzel, G. Mette, P. Stromberger, U. Koert, M. Dürr, U. Höfer, *J. Phys. Chem. C* **2015**, 119, 6018–6023.
- [40] F. Rochet, F. Jolly, F. Bournel, G. Dufour, F. Sirotti, J.-L. Cantin, *Phys. Rev. B* **1998**, 58, 11029–11042.
- [41] T. Glaser, C. Länger, J. Heep, J. Meinecke, M. G. Silly, U. Koert, M. Dürr, *J. Phys. Chem. C* **2020**, 124, 22619–22624.
- [42] J. Pecher, C. Schober, R. Tonner, *Chem. Eur. J.* **2017**, 23, 5459–5466.
- [43] L. Pecher, S. Laref, M. Raupach, R. Tonner, *Angew. Chem. Int. Ed.* **2017**, 56, 15150–15154; *Angew. Chem.* **2017**, 129, 15347–15351.
- [44] M. Raupach, R. Tonner, *J. Chem. Phys.* **2015**, 142, 194105.

Manuscript received: October 20, 2020

Revised manuscript received: November 25, 2020

Accepted manuscript online: December 1, 2020

Version of record online: January 21, 2021